Structured light-based 3D Reconstruction for Device of Minute Size

Jun Cheng[1], Ronald Chung[1], and Edmund Y. Lam[2]

[1] Dept. of Automation & Computer-Aided Engineering,
The Chinese Univ. of Hong Kong,
Hong Kong, China,
{jcheng, rchung}@acae.cuhk.edu.hk
[2] Dept. of Electrical & Electronic Engineering,
The Univ. of Hong Kong
Hong Kong, China
elam@eee.hku.hk

Abstract. In a previous work, we proposed a new binary-light projection mechanism that had a much reduced system size that made it particularly suitable for 3D shape inspection of semiconductor products. The mechanism is based upon the use of a light source and a binary grating for projecting a binary pattern, and of a camera for capturing image of the illuminated scene. By shifting the binary grating in space and in every shifting taking a separate image of the illuminated surface, each position on the illuminated surface will be attached with a string of binary code over the sequence of captured images. With a suitable design of the binary grating, the binary code string can be made unique for each bump surface position, allowing exact correspondence between the binary pattern and image data, and subsequently 3D determination through triangulation. In the mechanism the inspection speed is governed by the number of needed images which also equals the number of spatial shiftings of the grating. This paper addresses how the grating, as well as its spatial shifting, can be designed optimally for minimizing this image number for faster inspection speed. A closed-form solution to shifting strategy optimization is proposed that is applicable to any pattern on the fringe grating. A design method is also introduced for optimal pattern design, which has higher efficiency than brute-force searching. Theoretical analysis and real image experiments are presented to illustrate the workability of the solutions.

1 Introduction

In advanced electronic manufacturing that involves say die-to-die bonding, microscopic surfaces like solder bumps on wafers have to be inspected in 3D. Yet the tiny size and often highly specular and textureless nature of the surfaces make the task difficult. The size of the entire inspection system is also required to be small so as to minimize restraint on the operation of the various moving parts in the manufacturing process. There have been a few gray-level coding-based approaches proposed for 3D reconstruction, but as discussed in [1] they all suffer from problems of image noise and gray level saturation [2–5].

One way to counteract image noise and gray level saturation and alike problems is to replace the analog signals by discrete ones like binary signals. Binary pattern projection and imaging for 3D reconstruction is not a new idea. It has been explored under the name of structured light-based 3D reconstruction. Posdamer and Altschuler [6] and Altschuler, Altschuler and Taboada [7, 8] proposed the use of a pattern that consisted of a dot matrix of $n \times n$ binary light beams. Each column of the pattern could be independently controlled to be lighted or obscured, thus equipping the illuminated position on the target surface a binary code either '1' or '0'. By projecting a sequence of n patterns, they could encode 2^n stripes whose codewords were the sequence of 0's and 1's obtained from the n patterns. Inokuchi, Sato and Matsuda [9] furthered this encoding mechanism and proposed changing the binary codification to a Gray codification, which was more robust against noise for the Hamming distance of Gray code was one. Caspi et al. [10] proposed a multilevel Gray code based on color.

Yet, in traditional binary pattern projection the illumination pattern is meant to be an array of on-off controllable light sources like an LCD panel. As explained in [1], such arrangement is however not suitable for the inspection of the targeted devices because of the limitation of the system size. In a previous work [1] we proposed an alternative binary pattern projection mechanism. It was aimed at achieving an inspection device that is of small size yet capable of reconstructing a large area of the inspected surface. The mechanism uses a parallel or point light source in combination with a binary grating to allow a discrete pattern to be projected onto the inspected surface. As only a single light source is used the whole system is compact occupying only a small physical size. To change the binary pattern in every image snapshot, the binary grating is shifted in space with respect to the light source, the inspected surface, and the camera which are all kept stationary.

The challenge of the newly proposed mechanism is, while in the traditional binary projection approach the individual pattern elements (which are separate LCD light sources) can have their on-and-off's separately controlled, in the new mechanism they cannot. The bit values (1 or 0) of different positions of the pattern at any particular time are globally related to one another for the fact that the binary grating is constant, the light source is only one, and the change in pattern value is only induced by a physical and global shifting of the grating in space.

In other words, while in traditional binary projection approach it requires only $\log_2 N$ images to be taken to let N positions on the inspection surface have each a unique binary code, in the new approach it might require more, and the number $\log_2 N$ is only the lower bound. The important question is then how the binary pattern on the grating, as well as the shifting strategy which needs not one fringe at a time, could be designed to minimize the total number of images needed and make the number closer to $\log_2 N$. This paper addresses just that. A closed-form solution to shifting strategy optimization is proposed that is applicable to any binary pattern on the fringe grating. A design method is also introduced for optimal pattern design, which has great efficiency compared to brute-force searching. Theoretical analysis and real image experiments are also presented to illustrate the workability of the solutions.

The organization of the paper is as follows. In Section 2 we describe our codification strategy. Section 3 shows some experimental results. Concluding remarks are presented in Section 4.

2 Position Codification under Binary Fringe Grating in motion

The fringe grating could comprise regular pattern or irregular one. Fig. 1(b) illustrates one irregular pattern. Shifting a grating of period P several times is equivalent to dissecting the grating into several stripes which we refer to as the Grating-Motion Induced Zone (GZ). The more are the shifting times, the higher will be the column resolution. In order to reconstruct 3D surface with high speed, the projection pattern together with the shifting strategy should be optimized. An example of codification is shown in Fig. 1(a).

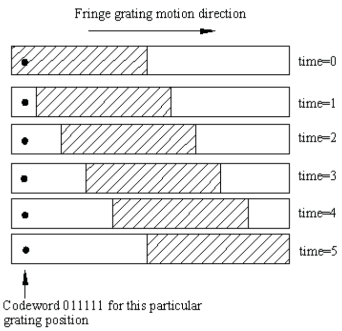

(a) An example of codeword production.

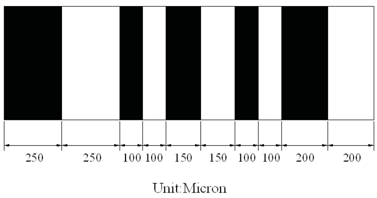

(b) Designed binary pattern.

Fig. 1. An example of codification mechanism and irregular pattern design.

2.1 Shifting strategy optimization of irregular pattern

Irregular pattern has richer encoding capacity than the regular pattern, allowing the need of less spatial shiftings of the fringe grating and in turn less imagings of the illuminated surface for creating unique binary codeword for each position of the inspected surface. The complication for irregular pattern is, adopting different combinations of the shifting steps could produce different sets of codewords with different lengths. Therefore, in order to produce a set of codewords with the shortest length, the shifting strategy has to be optimized. This part addresses the problem and gives a closed-form solution that is based on elementary matrix operations.

Given an irregular pattern P that comprises n GZs, we have $P = C_1 C_2 \cdots C_n$, where $C_i \in \{0, 1\}$, $i = 1, 2, \cdots, n$. There are at most n different shiftings:

$$\begin{cases} P_1 = C_1 C_2 \cdots C_{n-1} C_n \\ P_2 = C_n C_1 \cdots C_{n-2} C_{n-1} \\ \vdots \\ P_n = C_2 C_3 \cdots C_n C_1 \end{cases} \tag{1}$$

A subset of the above shiftings constitute a shifting strategy. The objective of the shifting strategy design is to use the minimum number of shiftings (and thus image number) to give each fringe grating position (which corresponds to a particular position on the inspected surface) a unique codeword.

We could use the following matrix to represent the information contained above:

$$M = \begin{pmatrix} C_1 & C_2 & \cdots & C_n \\ C_n & C_1 & \cdots & C_{n-1} \\ \vdots & & & \\ C_2 & C_3 & \cdots & C_1 \end{pmatrix} \tag{2}$$

Here the rows correspond to the various fringe grating positions, and the columns represent codewords related to those positions due to the composite effect of the shiftings.

The shifting strategy design problem is then about the determination of the smallest subset of M's rows (which correspond to the various shiftings P_i's) that allow the resultant partial columns (which correspond to the partial codewords) to be all different across the different fringe grating positions.

Codewords that are unique must have zero difference with any other codeword. Thus the difference matrix E affiliated with M, i.e., the matrix with columns being the differences between every pair of M's columns, can help solve the problem. The problem can thus be further degenerated into one that selects the minimum number of rows from the difference matrix E so that all the resultant sub-columns have at least one nonzero element.

We thus have the following shifting strategy optimization algorithm:
1. Construct the above $n \times n$ matrix M from the n patterns encapsulated in Equation (1):

2. Every column subtracts all the other columns. Thus a new matrix E can be obtained, whose size is $n \times l$ where $l = C_n^2$, and the elements are absolute values of difference:

$$E = \begin{pmatrix} |C_1 - C_2| \cdots & |C_1 - C_n| & |C_2 - C_3| \cdots & |C_2 - C_n| & \cdots & |C_{n-1} - C_n| \\ |C_n - C_1| \cdots & |C_n - C_{n-1}| & |C_1 - C_2| \cdots & |C_1 - C_{n-1}| & \cdots & |C_{n-2} - C_{n-1}| \\ \vdots & & & & & \\ |C_2 - C_3| \cdots & |C_2 - C_1| & |C_3 - C_4| \cdots & |C_3 - C_1| & \cdots & |C_n - C_1| \end{pmatrix} \quad (3)$$

Because $C_i \in \{0, 1\}$, the elements of matrix E will be in $\{0, 1\}$. '0' represents that the corresponding bits of the two codewords are the same, and '1' represents that they are different. The shifting strategy optimization problem can be described as the following: Select the minimum number of rows from matrix E to form a new matrix F such that the sum of every column of F is greater than zero. Every row of F can be selected from E step by step and in every step t one row is selected. Initially, $t = 1$, and $E^t = E$.

3. The size of matrix E^t is $n^t \times l^t$. Interchange the rows of matrix E^t to rearrange the rows so that the row sums are in descending order. Interchange the columns of matrix E^t to make all the elements '0' in the first row to be in the back of the matrix:

$$E^t = \begin{pmatrix} e^t_{i_1 j_1} & e^t_{i_1 j_2} & \cdots & e^t_{i_1 j_k} & e^t_{i_1 j_{k+1}} & \cdots & e^t_{i_1 j_{l^t - 1}} & e^t_{i_1 j_{l^t}} \\ e^t_{i_2 j_1} & e^t_{i_2 j_2} & \cdots & e^t_{i_2 j_k} & e^t_{i_2 j_{k+1}} & \cdots & e^t_{i_2 j_{l^t - 1}} & e^t_{i_2 j_{l^t}} \\ \vdots & & & & & & & \\ e^t_{i_{n^t} j_1} & e^t_{i_{n^t} j_2} & \cdots & e^t_{i_{n^t} j_k} & e^t_{i_{n^t} j_{k+1}} & \cdots & e^t_{i_{n^t} j_{l^t - 1}} & e^t_{i_{n^t} j_{l^t}} \end{pmatrix} \quad (4)$$

where $e^t_{i_1 j_1} = e^t_{i_1 j_2} = \cdots = e^t_{i_1 j_k} = 1$, $e^t_{i_1 j_{k+1}} = \cdots = e^t_{i_1 j_{l^t}} = 0$, and $\sum_{q=1}^{n^t} e_{q j_1} \geq \sum_{q=1}^{n^t} e_{q j_2} \geq \cdots \geq \sum_{q=1}^{n^t} e_{q j_{l^t}}$

The row number i_1^t in matrix E corresponding to the first row in matrix E^t will be one optimal shifting. Record it in the shifting strategy $S_{optimal}$. If all the elements in the first row equal to 1, i.e., $\prod_{q=1}^{l^t} e^t_{i_1 q} = 1$, then stop.

4. Set $t = t + 1$ and

$$E^t = \begin{pmatrix} e^{t-1}_{i_2 j_{k+1}} & \cdots & e^{t-1}_{i_2 j_{l^t - 1}} & e^{t-1}_{i_2 j_{l^t}} \\ \vdots & & & \\ e^{t-1}_{i_{n^{t-1}} j_{k+1}} & \cdots & e^{t-1}_{i_{n^{t-1}} j_{l^{t-1}} - 1} & e^{t-1}_{i_{n^{t-1}} j_{l^{t-1}}} \end{pmatrix}$$

Go to step 3.

$S_{optimal}$ will be one optimal shifting strategy. This closed-form solution could be used to obtain an optimal shifting strategy for any binary pattern.

2.2 Optimal irregular pattern design

In the new approach, one important question is how the binary pattern on the grating could be designed to minimize the total number of images needed. The optimal design objective is to design an irregular pattern, by which the minimal number of images can be achieved if combined with the shifting strategy optimization described above.

The problem can be viewed from the opposite end: for a fixed number of shiftings design a pattern with the maximum number of GZs . A conjecture about the optimal pattern is given in the following.

Conjecture: If the fixed number of shiftings is m, then the maximum length of the optimal pattern should be 2^m. Furthermore, the pattern comprises 2^{m-1} bits of 0 and 2^{m-1} bits of 1.

The conjecture has been verified correct empirically by experiments over a number of values of the shifting number m. Furthermore, we can prove that the pattern comprises 2^{m-1} bits of 0 and 2^{m-1} bits of 1.

Therefore, the optimization problem can be described as the following: Search for $C_1, C_2, \cdots, C_{2^m} \in \{0, 1\}$ and shift $p_1, p_2, \cdots, p_{m-1}$, such that:

$$\begin{cases} \sum_{i=1}^{2^m} C_i = 2^{m-1} \\ C_i C_{(i+p_1) \bmod 2^m} \cdots C_{(i+p_{m-1}) \bmod 2^m} \neq C_j C_{(j+p_1) \bmod 2^m} \cdots C_{(j+p_{m-1}) \bmod 2^m} \\ \forall i, j = 1, 2, \cdots, 2^m \quad i \neq j \end{cases} \tag{5}$$

A brute-force algorithm could be adopted to tackle the above. However, the size of the search space K_m, obtainable from Equation (6), will increase exponentially with the increase of the shifting number m. For example, if m is 6, the size of the search space is about 2.86×10^{16} which is huge.

$$K_m = \frac{1}{2^m} \sum_{d=1; d|2^{m-1}}^{2^{m-1}} \varphi(d) \frac{(2^m/d)!}{(2^{m-1}/d)!^2} \tag{6}$$

where

$$\begin{cases} \varphi(d) = d \left(\sum_{k=1;k|d}^{d} \frac{\mu(k)}{k} \right) \\ \mu(k) = \begin{cases} 1 & \mathrm{k} = 1 \\ (-1)^l & \text{if } \mathrm{k} = \mathrm{p_1 p_2 \cdots p_l}, \text{ where the } \mathrm{p_i} \text{ are distinct primes.} \\ 0 & \text{others} \end{cases} \end{cases}$$

The problem expressed by Equation (5) could be converted to this: Find 2^{m-1} indexes $i_1, i_2, \cdots, i_{2^{m-1}}$ for 2^{m-1} bits of 1 and $m-1$ shiftings of $p_1, p_2, \cdots, p_{m-1}$, such that:

$$\begin{cases} |S_{j_1} \bigcap S_{j_2} \bigcap \cdots \bigcap S_{j_t}| = 2^{m-t} & \mathrm{t} = 1, 2, \cdots, \mathrm{m} \\ |\bigcup_{k=0}^{m-1} S_k| = 2^m - 1 \end{cases} \tag{7}$$

where $|\cdot|$ is the size of a set.

$$\begin{cases} S_0 = \{i_1, i_2, \cdots, i_{2^{m-1}}\} \\ S_j = \{(i_1 + p_j) \bmod 2^m, (i_2 + p_j) \bmod 2^m, \cdots, (i_{2^{m-1}} + p_j) \bmod 2^m\} \\ \qquad \mathrm{j} = 1, 2, \cdots, \mathrm{m} - 1 \end{cases}$$

An irregular pattern is composed of several basic cells. A basic cell (**BC**) is a set which comprises a number of continuous bits of 0 and a number of continuous bits of 1. From Equation (7), all the BCs of one optimal pattern could be obtained if we set $p_1, p_2, \cdots, p_{m-1}$ to be $\{1, 2, \cdots, m-1\}$.

$$BCs = \left\{ \begin{array}{c} \underbrace{0\cdots0}_{m}\underbrace{1\cdots1}_{m}, \underbrace{0\cdots0}_{m-1}1, \cdots, \overbrace{\underbrace{0\cdots0}_{m-k}\underbrace{1\cdots1}_{k-j}, \cdots, \underbrace{0\cdots0}_{m-k}\underbrace{1\cdots1}_{k-j}}^{2^{j-2}}, \\ \cdots, \overbrace{\underbrace{0\cdots0}_{m-k}1, \cdots, \underbrace{00\cdots0}_{m-k}1}^{2^{k-3}}, \cdots \end{array} \right\}$$

Knowing all the BCs, the optimal pattern could be obtained by checking every combination of these BCs. The size of the search space will be $\frac{2^{m-2}!}{\prod_{k=3}^{m-1}\prod_{j=2}^{k-1} 2^{j-2}!}$. Therefore, the size of the search space is reduced substantially from that of the original search space. For example, if $m = 6$, the size of the search space now is about 2.18×10^{10}, which is reduced by 1.31×10^{6} times from the original one. Optimized irregular pattern requires only $\log_2 N$ images to be taken to let N positions on the inspection surface have each a unique binary code, while regular pattern requires $N/2$ images.

3 Experiments

We have implemented the proposed system and tested it with a designed pattern (Fig. 1(b)) of period $1600\mu m$. The grating was projected by the use of a projector onto the surface at an inclination angle of 30 degree. The scene was grabbed by a CCD camera through microscopy. In order to demonstrate that the irregular pattern has the ability of enlarging measurement range significantly, the pattern was used to reconstruct a wafer whose height was about $400\mu m$ and a relatively large free-form object whose height was about 3mm.

The pattern could be divided into 32 GZs. Because of the limitation of our projector's bandwidth, the minimal stripe that could be projected by the projector comprises 2 GZs. Therefore, the images needed was greater than the lower bound. 6 images are enough to produce unique codeword. In order to make the system more robust, a suboptimal shifting strategy including 7 shiftings was adopted.

$$\begin{pmatrix}
0&0&0&0&0&1&1&1&1&1&0&0&1&1&0&0&0&1&1&1&0&0&1&1&0&0&0&0&1&1&1&1\\
1&0&0&0&0&0&1&1&1&1&1&0&0&1&1&0&0&0&1&1&1&0&0&1&1&0&0&0&0&1&1&1\\
1&1&0&0&0&0&0&1&1&1&1&1&0&0&1&1&0&0&0&1&1&1&0&0&1&1&0&0&0&0&1&1\\
0&1&1&1&1&0&0&0&0&0&1&1&1&1&1&0&0&1&1&0&0&0&1&1&1&0&0&1&1&0&0&0\\
0&0&0&1&1&1&1&0&0&0&0&0&1&1&1&1&1&0&0&1&1&0&0&0&1&1&1&0&0&1&1&0\\
0&0&0&0&1&1&1&1&0&0&0&0&0&1&1&1&1&1&0&0&1&1&0&0&0&1&1&1&0&0&1&1\\
1&0&0&1&1&0&0&0&0&1&1&1&1&0&0&0&0&0&1&1&1&1&1&0&0&1&1&0&0&0&1&1
\end{pmatrix}$$

Fig. 2 shows operation image sequence and 3D result of the wafer. To illustrate the larger measurement range of the irregular pattern, we performed an experiment on a relatively large free-form object. Fig. 3 shows the operation image sequence and 3D result. The results show that the optimal irregular pattern in combination with the optimal shifting strategy allow less image number to be used than the regular pattern. In order to maintain the same measurement range and x-y resolution, 17 images are to be required if regular pattern is adopted.

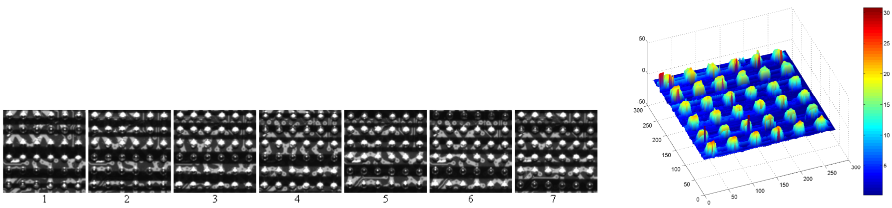

(a) Image sequence of wafer in the operation phase. (b) 3D reconstruction.

Fig. 2. Experiment on wafer with irregular pattern.

4 Conclusion and Future Work

We have presented a 3D reconstruction approach that projects binary pattern through the use of a binary fringe grating which is to be shifted spatially. To increase the the measurement range and reduce the image number needed, a closed-form solution to shifting strategy optimization based on elementary matrix operations has been proposed. The solution is applicable to any binary pattern. A design method is also introduced for optimal pattern design, which has higher efficiency than brute-force searching. By the optimal design, our system requires only $\log_2 N$ images to be taken to let N positions on the inspection surface have each a unique binary code, which is the same as that of the traditional binary pattern projection approach. Experiments on a wafer and a relatively large free-form object with irregular pattern demonstrate that the optimized pattern and shifting strategy could have relatively large measurement range and small image number.

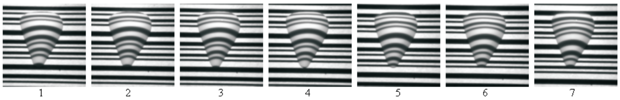

(a) Image sequence of inspected surface in the operation phase.

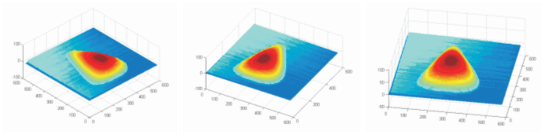

(b) 3D reconstruction of the inspected surface, as observed from different angles.

Fig. 3. Experiment on free-form object with irregular pattern.

ACKNOWLEDGMENT The work described in this paper was substantially supported by a grant from the Innovation and Technology Commission of Hong Kong Special Administrative Region, China, under an Innovation and Technology Fund with Project Code UIM/111.

References

1. Cheng, J., Chung, R., Lam, E., Fung, K., Wang, F., Leung, W.: Three-dimensional reconstruction of wafer solder bumps using binary pattern projection. Volume 5679 of Proc. SPIE. (2005) 44–52
2. Takasaki, H.: Moire topography. Applied Optics **9** (1970) 1467–1472
3. Kim, S., Choi, Y., Oh, J.: Three-dimensional profile measurement of fine object by phase-shifting moiré interferomety. Volume 2909 of Proc. SPIE. (1997) 28–36
4. Wust, C., Capson, D.W.: Surface profile measurement using color fringe projection. Machine Vision Application **4** (1991) 193–203
5. Huang, P.S., Zhang, C.P., Chiang, F.P.: High speed 3-d shape measurement based on digital fringe projection. Optical Engineering **42(1)** (2003) 163–168
6. Posdamer, J.L., Altschuler, M.: Surface measurement by space-encoded projected beam systems. Computer Graphics and Image Processing **18(1)** (1982) 1–17
7. Altschuler, M.D., Altschuler, B.R., Dijak, J.T., Tamburino, L.A., Woolford, B.: Robot vision by encoded light beams. In Kanade, T., ed.: Three-Dimensional Machine Vision. Kluwer Academic, Dordrecht (1987) 53–71
8. Altschuler, M.D., Altschuler, B.R., Taboada, J.: Laser electro-optic system for rapid three-dimensional (3-d) topographic mapping of surfaces. Optical Engineering **20(6)** (1981) 953–961
9. Inokuchi, S., Sato, K., Matsuda, F.: Range-imaging for 3-d object recognition. Proc. Int. Conf. on Pattern Recognition (1984) 806–808
10. Caspi, D., Kiryati, N., Shamir, J.: Range imaging with adaptive color structured light. IEEE Trans. Pattern Anal. Mach. Intell. **20(5)** (1998) 470–480